

# International Cometary Explorer Encounter with Giacobini-Zinner: Magnetic Field Observations

EDWARD J. SMITH, BRUCE T. TSURUTANI, JAMES A. SLAVIN,  
DOUGLAS E. JONES, GEORGE L. SISCOE, D. ASOKA MENDIS

The vector helium magnetometer on the International Cometary Explorer observed the magnetic fields induced by the interaction of comet Giacobini-Zinner with the solar wind. A magnetic tail was penetrated  $\sim 7800$  kilometers downstream from the comet and was found to be  $10^4$  kilometers wide. It consisted of two lobes, containing oppositely directed fields with strengths up to 60 nanoteslas, separated by a plasma sheet  $\sim 10^3$  kilometers thick containing a thin current sheet. The magnetotail was enclosed in an extended ionosheath characterized by intense hydromagnetic turbulence and interplanetary fields draped around the comet. A distant bow wave, which may or may not have been a bow shock, was observed at both edges of the ionosheath. Weak turbulence was observed well upstream of the bow wave.

**M**AGNETIC FIELD MEASUREMENTS near comets are of scientific interest because they represent an important aspect of the interaction of the comet with the solar wind and should reveal how the comet becomes magnetized. When an active comet is observed, it has already developed a structure that is dependent on the presence of magnetic fields derived from the solar wind, the most obvious manifestation being the magnetic field in the ion tail. In the absence of direct observations, competing theories (1) often provide several possible answers to issues such as (i) the existence of a bow shock that accompanies the comet as it moves through the inner solar system; (ii) the number, character, and length scales of different plasma regimes surrounding the comet; and (iii) the strength of the magnetic field in the coma and tail.

The encounter with Giacobini-Zinner provided an opportunity to address these and other important issues. The experiment complement on the International Cometary Explorer (ICE) included a vector helium magnetometer (2). Throughout the encounter, the scientific data were telemetered at a rate equivalent to a vector field measurement each  $1/3$  second and to a spatial resolution of 7 km. The instrument had more than adequate sensitivity (0.01 nT) and dynamic range (a capability to measure maximum fields in excess of  $10^5$  nT), and it performed faultlessly. Instrument performance did not influence the data acquired.

The first obvious evidence of the approaching comet (Fig. 1) was the spacecraft's entry into a region characterized by extreme hydromagnetic turbulence that was unlike the usual interplanetary field irregularities. In Fig. 1 and in the other figures the field components are shown in coordinates based on the ICE spin axis and the direction to the sun (I,S coordinates). These coordinates are almost identical with the solar

ecliptic coordinates  $x$ ,  $y$ , and  $z$ , where  $x$  is sunward,  $z$  points to the north ecliptic pole, and  $y$  is opposite the direction of planetary motion. Since the interplanetary field tends to be parallel to the ecliptic plane on the average, these coordinates are suitable for the preliminary analysis reported here. The turbulence involved random changes in the field components that were comparable in magnitude to that of the background or average field (Fig. 2). Localized packets of relatively high-frequency fluctuations (typical periods,  $\sim 3$  second) were interspersed at irregular intervals within the large variations in amplitude. In retrospect, the interplanetary field was seen to become irregular at even larger distances from Giacobini-Zinner, but the changes were smaller in amplitude and less readily noticeable.

Entry into this turbulent region appeared to be gradual. The average field strength rose to  $\sim 15$  nT over an interval of about 10 minutes from the interplanetary value of 8. The transition occurred at 09:30 universal time (U.T.), or about 1.5 hours before closest approach. Inspection of the data (1-minute averages) showed only a gradual increase in field strength, and the transition did not have the usual appearance of a collisionless bow shock. At the time of observation, the average interplanetary field orientation corresponded fairly well to the average Parker spiral with the addition of a significant southward component. This field orientation would have been consistent with a quasi-perpendicular shock, so that the absence of an abrupt jump in the magnetic field could not be attributed to the shock being quasi-parallel. Careful analysis, including correlative studies with the other ICE measurements, will have to be carried out to determine whether or not a shock was observed. For now, we characterize the transition simply as a bow wave accompanying the comet.

The region between the bow wave and

the magnetic tail, which we designate the ionosheath, was observed on the spacecraft's inbound trajectory for 1.5 hours (Fig. 1). Average field strength rose toward the middle of the interval to a maximum of about 25 nT. The average field orientation, which continued to be outward and southward, was consistent with draping of the sheath magnetic field lines around the comet. The increase in field strength was, presumably, a manifestation of a gradual compression of the plasma as its flow speed decreased toward the tail axis (3).

Intermittently, the spacecraft encountered sheath regions that differed from the surrounding plasma in that the field was both weaker (typically  $\sim 5$  nT) and quieter (lower amplitude field fluctuations). One such low-field region was observed just before 11:00 U.T., adjacent to the magnetotail (Fig. 3). When the spacecraft was roughly midway through the region, the field direction reversed, changing from a draped outward-directed field to an inward-directed field. A plausible explanation is that a folded field line was being observed downstream from some obstacle, other than the inner coma, around which it was draped. Two low-field regions may be seen at earlier times; however, examination of these regions has not revealed the strong reversal in direction that characterized the example above. Several examples of low-field regions could also be seen outbound. There was a hint of a periodicity of  $\sim 30$  minutes, possibly associated with the rotation of the nucleus or with the plasma interaction.

The spacecraft passed from the low-field region observed just before closest approach directly into the magnetotail of Giacobini-Zinner (Fig. 4). We identify the relatively abrupt increase in the field magnitude,  $B$ , at 10:59:40 U.T. with entry into the tail. The field magnitude rose rapidly to a maximum of 60 nT while the direction became distinctly more tail-like, although not strictly antisunward. The current sheet (not strictly a "neutral sheet" because  $B \neq 0$ ) was then penetrated, as evidenced by the abrupt drop in  $B$  to about 5 nT. The current sheet was traversed in 1 minute and the spacecraft entered the magnetic lobe of opposite polarity in which  $B$  again rose rapidly to a value of 60 nT. Exit from the magnetotail occurred at 11:07:40 U.T., at which time there was

E. J. Smith, B. T. Tsurutani, J. A. Slavin, Jet Propulsion Laboratory, California Institute of Technology, Pasadena, CA 91109.

D. E. Jones, Department of Physics and Astronomy, Brigham Young University, Provo, UT 84601.

G. L. Siscoe, Department of Atmospheric Sciences, University of California, Los Angeles, CA 90024.

D. A. Mendis, Department of Electrical Engineering and Computer Sciences, University of California at San Diego, La Jolla, CA 92093.

an abrupt decrease in  $B$  to levels characteristic of the spacecraft's outbound traversal through the plasma sheath on the opposite side of the tail. Inspection of the field changes during the tail crossing revealed a few examples of what may have been a return to the lobe configuration or brief entries of the spacecraft into the current sheet. These excursions may be explained either as filamentary tail structure or as a flapping or waving intrinsic to the tail (as is commonly observed in Earth's magnetotail).

The character of the sheath on the spacecraft's outbound trajectory was similar to that observed on the inbound trajectory. A high level of hydromagnetic turbulence was punctuated by occasional passages through low-field regions. The sheath was observed until either 12:01 or 12:20 U.T., both times being associated with decreases in  $B$ , which might be considered to be the bow wave (Fig. 1). In either case, the duration of the sheath outbound was roughly comparable to its duration inbound (1.0 compared to 1.5 hours). From 12:20 U.T. on, the spacecraft appeared to have returned to the relatively undisturbed solar wind, although weak turbulence persisted well upstream from the bow wave. Either of the above decreases in field strength might be interpreted as a bow shock (both may be explained this way, since the heavy cometary ions might produce a unique shock structure). An alternative explanation is that at least one of them represents a discontinuity in the interplanetary magnetic field that occurred while the spacecraft was still in the sheath.

The question of whether or not the bow wave is a shock was pursued initially by plotting the inbound and outbound measurements at high time resolution (Fig. 5). The most obvious feature of both crossings was the onset of strong turbulence at 09:30 U.T. and its even more abrupt cessation at 12:20 U.T. The field magnitude contained pulsations as large as the average field and with maxima many times larger than the minima (possibly the background field). If these structures are shocks, their appearance is unlike any planetary bow shocks of which we are aware. On the other hand, there are reasons for expecting a cometary shock to be different from planetary shocks owing to the heavy cometary ions loaded into the upstream solar wind. Further analysis of these and the simultaneous plasma (3) and plasma wave (4) data will be required to determine whether the bow wave is a shock.

The observations before and after the encounter provide the basis for ascertaining whether significant changes occurred in the solar wind while the spacecraft was inside the cometary interaction region. The field

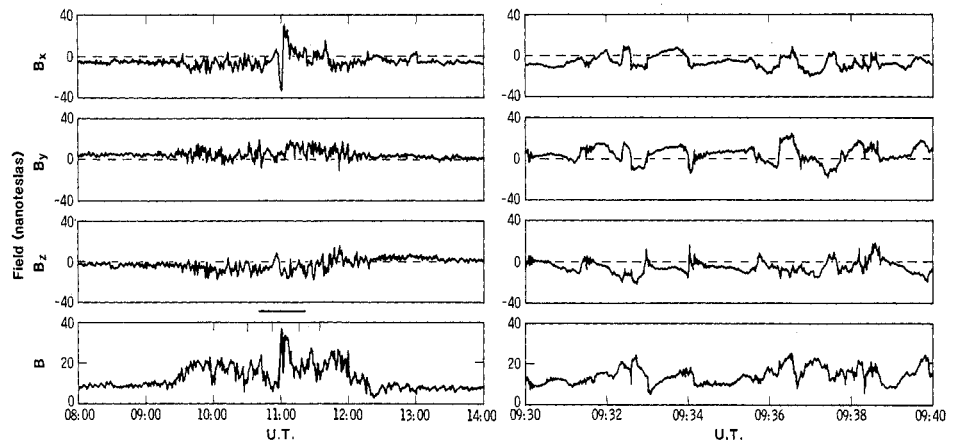


Fig. 1 (left). Overview of magnetic field observations in the vicinity of Giacobini-Zinner. The field magnitude and three components are shown for 6 hours centered on closest approach. The solid horizontal bar above the bottom panel corresponds to a scale of  $10^5$  km (the diameter of the visible coma). The vertical tick marks along the upper edge of this panel identify low-field regions. Fig. 2 (right). Example of hydromagnetic fluctuations in the ionosheath. The field magnitude and three components are shown during a 10-minute interval. Each field vector, measured every 0.33 second, is displayed. The long period ( $\sim 1$ -minute) variations have large amplitudes, with changes in the components that are comparable to the average magnitude ( $\Delta B/B$ ,  $\sim 1$ ).

observations indicate that Giacobini-Zinner was immersed in an interplanetary field that was pointing out from the sun (conventionally described as a positive magnetic sector) throughout the encounter. The solar wind analyzer measurements indicate that the encounter occurred in the trailing portion of a recurrent high-speed stream (3). This circumstance would normally be fortunate from the standpoint of not having to cope with large changes in the solar wind. The trailing part of high-speed streams is generally relatively structureless and exhibits a gradual decline in speed and temperature

with perhaps a slight increase in density. The interplanetary field also tends to be relatively free of large discontinuities, heliospheric current sheet crossings, or other major changes in field orientation or magnitude. However, comparison of the magnetic data from before and after the encounter shows that the orientation of the field did change. The change was associated principally with the north-south component, which was southward before the encounter and north afterward.

From the major features of the cometary interaction, it is possible to invoke a symme-

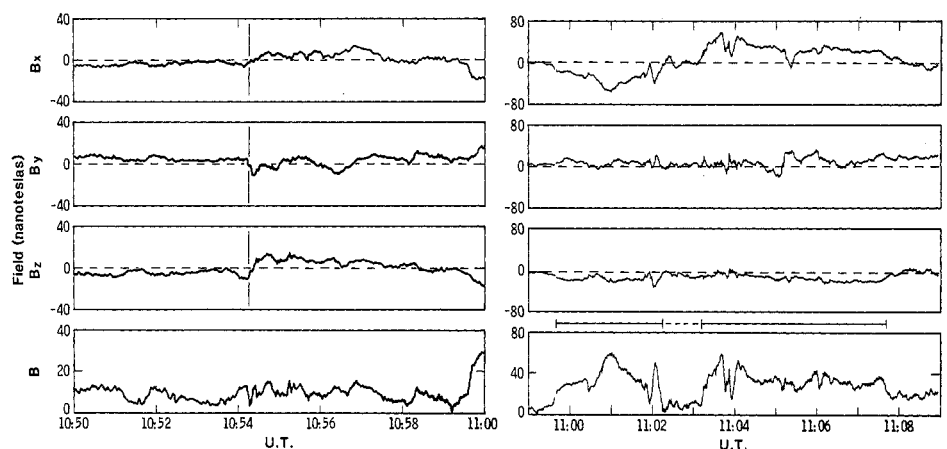


Fig. 3 (left). Field reversal in the low-field region adjacent to the magnetotail. Each measured field vector and its magnitude are shown over a 10-minute interval centered on the field reversal at 10:54:20 U.T. The  $B_x$  and  $B_z$  components change sign at that time and return to their normal orientation at 10:59:40 U.T., when the boundary of the tail is crossed. Fig. 4 (right). Observations of the magnetotail. The magnitude and components of the individual vectors are displayed from entry into the tail (10:59:40 U.T.) until exit (11:07:40 U.T.). The horizontal line above the lower panel identifies this region. The reversal in field direction (see  $B_x$ ) occurred at about 11:03 U.T. when  $B$  dropped to very low values. This current sheet crossing is identified by the dashed segment of the horizontal bar above  $B$ . Maximum  $B$  in the two lobes is 60 nT.

try between the inbound and outbound observations in order to infer when the interplanetary field may have changed direction. Draping of the field lines would be expected to reverse the radial field component while leaving the azimuthal and meridional components relatively unchanged. The observations show the expected reversal in the radial field component,  $B_x$ , on crossing the magnetic tail. The north-south component,  $B_z$ , had a southward orientation after the magnetotail crossing until 11:42 U.T., when it became northward and  $B_x$  simultaneously changed sign. We associate this time with a major change in the interplanetary field direction that reoriented the draped fields in the outbound ionosheath.

The identification of the various features above establishes some of the basic scale lengths associated with the comet-solar wind interaction. By using the times at which the features were observed and the spacecraft's velocity relative to Giacobini-Zinner of  $21 \text{ km sec}^{-1}$ , we can derive the following scales. The widths of the sheath inbound (1 hour, 30 minutes) and outbound (1 hour, 2 minutes) were 110,000 and 78,000 km, respectively. The magnetotail was 10,800 km wide (based on an interval of 8.0 minutes) and the plasma sheet, 1260 km (1.0 minutes). However, allowance should be made for the anticipated sheet-like structure of the current and its probable large inclination to the spacecraft's trajectory. Thus, if the current sheet was oriented  $45^\circ$  relative to the spacecraft's direction, this estimate would be decreased to about 900 km. If the current sheet was in motion, it could have passed the spacecraft with a speed different from that assumed, which would also affect these estimates.

Two observed asymmetries may be significant. The ionosheath is wider inbound than outbound by a factor of 1.4. The magnetotail crossings are asymmetric with respect to the current sheet, being 160 seconds (3360 km) inbound and 270 seconds (5670 km) outbound, a ratio of 1.7. Without further analysis, it is uncertain whether to attribute such differences to structure or time variations.

Since the upstream solar wind is definitely supersonic, the absence of a bow shock would be surprising. Such a result is consistent, however, with the suggestion that no bow shock occurs because solar wind pickup of heavy cometary ions causes a gradual, rather than an abrupt, transition to subsonic flow (5). Of course, a negative result downstream from the comet would not necessarily imply that the bow wave is not a shock in the subsolar region. The shock may simply have decayed away on the flanks, as proposed recently (6). The alternative, a well-

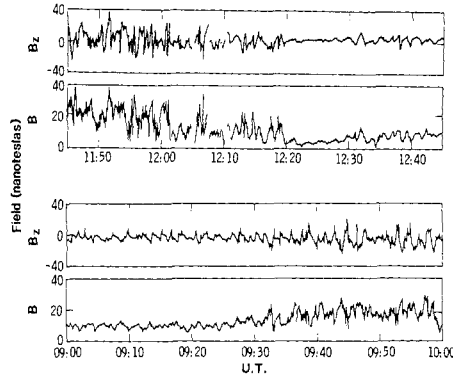


Fig. 5. Details of the bow wave inbound and outbound. The lower and upper panels contain the field magnitude and  $B_z$  for the inbound and outbound crossings, respectively. Only one component is shown because the others are basically very similar in character. Each plotted point is an average over the spacecraft spin period (3 seconds). The use of averages allows reasonably long intervals to be plotted.

defined shock on the flanks, has also been suggested (7).

The magnetic field variations in and upstream from the sheath include two distinctly different characteristic periods near 3 and 100 seconds. The two wave types appear to be coupled, with the shorter period wave packets seeming to occur near decreases in  $B$  associated with the longer period waves. The waveforms are reminiscent of those seen near Earth in the region upstream from the bow shock between noon and dawn in which ions reflected from the shock escaping upstream from the magnetosheath exert a strong influence on the impinging solar wind (8). It is tempting to identify the two characteristic periods with ion cyclotron resonances, the shorter period with light ions ( $H^+$ ) and the longer period with heavy ions [such as  $H_2O^+$ , the dominant cometary ion as observed by the ICE ion composition experiment (9)]. In a field of 10 nT, the gyroperiods of  $H^+$  and  $H_2O^+$  are 6 and 110 seconds, respectively.

The observation of kinked or folded field lines, as in the low-field region adjacent to the southern magnetic lobe, can be interpreted as a draping over an obstacle other than the central coma, which presumably gives rise to the long magnetic tail. Various possibilities can be entertained: the nucleus is fragmented and actually consists of two or more pieces; the nucleus is emitting gas sporadically and the obstacle is a gas jet of some sort; the draped fields have been able to slide around or under the cometary obstacle and are about to accelerate downstream to rejoin the solar wind; the folded field is a remnant of reconnected field associated with an earlier reversal in the interplanetary field;

or the field lines are working their way into the coma (perhaps by virtue of a basic mechanism such as the interchange or flute instability) and will eventually form part of the tail lobe.

The draping of the interplanetary field to form the magnetotail is similar to what is observed at Venus (10). However, the maximum field strength of 60 nT observed in both lobes is very different from that at Venus, where the tail field is more nearly equal to the interplanetary value (11). The strong field is probably the result of making observations within the coma of Giacobini-Zinner, and the field may be nearer the interplanetary value well downstream (12). Evidently the comet is efficient at capturing solar wind magnetic fields. It may be more than coincidence that the pressure of the maximum field strength is nearly equivalent to that required to hold off the incident solar wind, that is, the stagnation field.

Another interesting aspect of the magnetic field strength is the occurrence of the maximum toward the center of the lobe well away from the tail boundary and the current sheet. Viewed from the perspective of the currents responsible for this field configuration, volume currents within the lobes, rather than just surface currents along the boundaries (as at Earth), are implied. The existence of volume currents indicates that stresses are being exerted on most of the tail in addition to those at the bounding surfaces. The nature and origin of these stresses require further investigation, although one possibility is a significant nonuniform tension exerted on the draped field lines.

The fields in the lobes and current sheet exhibit a significant cross-tail component tending to point in approximately the  $y$  direction (opposite the motion of the spacecraft around the sun). The existence of this component has several important consequences. It shows that the field lines are not truly oppositely directed (corresponding to an angular difference of  $180^\circ$ ), but are somewhat flared. The flaring of the field lines is presumably an important aspect of the manner and rate at which magnetic flux is being added to the tail or possibly pulled through the coma. The flaring is expected to cause the field strength in the tail to be significantly smaller at larger distances downstream.

A point of physical interest is the ability of the plasma sheet, which contains the current sheet, to withstand the inward magnetic pressure being exerted by the lobe fields. A static pressure balance would require that the pressure of the plasma in the plasma sheet compensate for the pressure differential between the strong field in the lobe,  $B_L$ , and the weak field in the plasma sheet,  $B_P$ , of  $(B_L^2 - B_P^2)/8\pi \approx (B_L^2/8\pi) \approx (60 \times 10^{-5})^2/$

$8\pi = 1.4 \times 10^{-8}$  dyne  $\text{cm}^{-2}$  or  $9 \times 10^3$  eV  $\text{cm}^{-3}$ . The ICE radio astronomy investigation derived a measure of electron density ( $670 \text{ cm}^{-3}$ ) and temperature ( $1.3 \times 10^4$  K) in the current sheet from the plasma noise spectrum (13). The corresponding electron pressure is  $750 \text{ eV cm}^{-3}$ , which is substantially less than is needed to balance the magnetic pressure. If the additional pressure is provided by ions, they must be significantly hotter than the electrons; that is, their pressure must be 11 times larger, so that the ion temperature,  $T_i$ , is  $14.3 \times 10^4$  K or 12 eV. Alternatively, a small density ( $\sim 10 \text{ cm}^{-3}$ ) of hot electrons ( $\sim 1$  keV) could supply the needed pressure.

#### REFERENCES AND NOTES

1. Modern theories are based on outgassing of neutral molecules from a solid nucleus composed principally of dust and ices. The neutrals become ionized by solar radiation and charge exchange with solar wind protons and are then picked up by the magnetized solar wind. Two recent reviews are by D. A. Mendis and H. L. F. Houpsis [*Rev. Geophys. Space Phys.* **20**, 885 (1982)] and W.-H. Ip and W. I. Axford (7).
2. A. M. A. Frandsen *et al.*, *IEEE Trans. Geosci. Electron.* **GE-16**, 195 (1978).
3. S. J. Bame *et al.*, *Science* **232**, 356 (1986).
4. F. L. Scarf *et al.*, *ibid.*, p. 377.
5. M. K. Wallis, *Nature (London) Phys. Sci.* **233**, 23 (1971).
6. ——— and M. Dryer, *Nature (London)* **318**, 646 (1985).
7. W.-H. Ip and W. I. Axford, in *Comets*, L. Wilkening, Ed. (Univ. of Arizona Press, Tucson 1982), p. 588.
8. M. M. Hoppe, C. T. Russell, L. A. Frank, T. E. Eastman, E. W. Greenstadt, *J. Geophys. Res.* **86**, 4471 (1981).
9. K. Ogilvie *et al.*, *Science* **232**, 374 (1986).
10. C. T. Russell *et al.*, in *Comets*, L. L. Wilkening, Ed. (Univ. of Arizona Press, Tucson, 1982), p. 561.
11. J. A. Slavin, E. J. Smith, D. Intriligator, *Geophys. Res. Lett.* **11**, 1074 (1984).
12. A. I. Ershkovitch, *Mon. Not. R. Astron. Soc.* **184**, 755 (1978).
13. N. Meyer-Vernet *et al.*, *Science* **232**, 370 (1986).
14. We are grateful for the excellent support provided by members of the GSFC project, specifically T. von Roseninge, P. Corrigan, B. Wales, R. Farquhar, J. Brandt, and M. Niedner. J. Green, J. King, and their staff at NASA Space Science Data Center operated the Space Physics Analysis Network, which enabled us to transfer raw and reduced data back and forth across the United States. Key Jet Propulsion Laboratory personnel were B. Connor, A. Frandsen, J. Van Amerfoort, and J. Wolf. Portions of the work described were carried out at JPL, California Institute of Technology, under contract with NASA.

20 November 1985; accepted 6 February 1986

## Neoplastic Conversion of Human Keratinocytes by Adenovirus 12–SV40 Virus and Chemical Carcinogens

JOHNG S. RHIM, JUN FUJITA, PAUL ARNSTEIN, STUART A. AARONSON

Efforts to investigate the progression of events that lead human cells of epithelial origin to become neoplastic in response to carcinogenic agents have been aided by the development of tissue culture systems for propagation of epithelial cells. In the present study, nontumorigenic human epidermal keratinocytes immortalized by adenovirus 12 and simian virus 40 (Ad 12–SV40) were transformed by treatment with the chemical carcinogens *N*-methyl-*N'*-nitro-*N*-nitrosoguanidine or 4-nitroquinoline-1-oxide. Such transformants showed morphological alterations and induced carcinomas when transplanted into nude mice, whereas primary human epidermal keratinocytes treated with these chemical carcinogens failed to show any evidence of transformation. This *in vitro* system may be useful in assessing environmental carcinogens for human epithelial cells and in detecting new human oncogenes.

IT IS NOW ACCEPTED WIDELY THAT cancer arises in a multistep fashion and that environmental exposures, particularly to chemical, physical, and biological agents, are major etiological factors (1–3). The malignant transformation of human cells in culture by carcinogenic agents permits analysis of alterations and evolution in cell properties that may be representative of cancer cells. Although most models of neoplastic transformation of human cells *in vitro* by carcinogenic agents were based on the use of fibroblasts, which are easy to culture (4–11), neoplastic transformation of human skin fibroblasts in culture has not been readily achieved. Infection by certain DNA tumor viruses and, rarely, by chemical carcinogens has led to the development of established, karyologically abnormal lines of fibroblasts that are tumorigenic in suitable experimental models. Since most human tumors are of epithelial origin, it is important to study such cell systems. However, because of the inability until recently to grow epithelial cells and subsequently transformed human epithelial cells *in vitro*, it has

been difficult to study the genetic alterations involved in the process of malignant transformation of human epithelial cells. Although epithelial cell cultures derived from numerous organs of rodent model systems (12–16) have been neoplastically transformed by chemical carcinogens, there are few reports describing carcinogen-induced transformation of human epithelial cell cultures (17–19).

We recently developed an *in vitro* multistep model for human epithelial cell carcinogenesis (20). Primary human epidermal keratinocytes acquired an indefinite lifespan in culture but did not undergo malignant conversion in response to an adenovirus 12–simian virus 40 (AD 12–SV40) hybrid. The addition of Kirsten murine sarcoma virus (Ki-MSV), which contains a *K-ras* oncogene, to these cells induced striking morphological alterations and led to the acquisition of neoplastic properties (20). The availability of a human epithelial cell line that could undergo neoplastic conversion in response to a *ras* oncogene led us to inquire whether this system might be useful in

detecting chemical carcinogens for human epithelial cells.

Primary human foreskin epithelial cells were initiated in NCTC 168 medium with 10 percent horse serum containing antibiotics (gentamicin, 100  $\mu\text{g/ml}$ , and fungizone, 25  $\mu\text{g/ml}$ ) (21). The human epidermal keratinocyte line, designated RHEK-1, was established from primary human foreskin epidermal keratinocytes after they had been infected with Ad 12–SV40 virus (20). This line did not produce virus, had a "flat" epithelial morphology, and possessed a number of markers associated with epithelial cells. The line contained SV40 tumor antigens but was not tumorigenic in nude mice. Growth and maintenance medium consisted of Dulbecco's modified minimum essential medium (DMEM) with 15 percent fetal bovine serum (FBS), hydrocortisone (HC; 5  $\mu\text{g/ml}$ ), and antibiotics (gentamicin, 100  $\mu\text{g/ml}$ , and fungizone, 25  $\mu\text{g/ml}$ ) (DMEM + 15 percent FBS + HC).

After exposure of primary human epidermal keratinocytes to various doses of the chemical carcinogens *N*-methyl-*N'*-nitro-*N*-nitrosoguanidine (MNNG) or 4-nitroquinoline-1-oxide (4NQO), no morphological differences between treated and control untreated cultures could be seen. Neither control nor treated cultures were able to grow serially beyond two to three subcultures. The cells underwent progressive deterioration and were lost. In the RHEK-1 line exposed to MNNG at either 0.1 or 0.01  $\mu\text{g/ml}$ , morphological alterations of cells and an abnormal pattern of growth were noted by the sixth subculture, 52 to 62 days after treatment; similar changes were not observed in the control RHEK-1 cells treated with dimethylsulfoxide (DMSO).

Laboratory of Cellular and Molecular Biology, National Cancer Institute, Bethesda, MD 20892.